PROCEEDINGS OF SCIENCE

Cosmic-ray acceleration in supernova shocks

Vincent Tatischeff[*†]
Institut de Ciències de l'Espai (CSIC-IEEC), Campus UAB, Fac. Ciències, 08193 Bellaterra, Barcelona, Spain
E-mail: Vincent.Tatischeff@csnsm.in2p3.fr

Galactic cosmic rays are widely believed to be accelerated in expanding shock waves initiated by supernova explosions. The theory of diffusive shock acceleration of cosmic rays is now well established, but two fundamental questions remain partly unanswered: what is the acceleration efficiency, i.e. the fraction of the total supernova energy converted to cosmic-ray energy, and what is the maximum kinetic energy achieved by particles accelerated in supernova explosions? Recent observations of supernova remnants, in X-rays with the *Chandra* and *XMM-Newton* satellites and in very-high-energy γ rays with several ground-based atmospheric Cerenkov telescopes, have provided new pieces of information concerning these two questions. After a review of these observations and their current interpretations, I show that complementary information on the diffusive shock acceleration process can be obtained by studying the radio emission from extragalactic supernovae. As an illustration, a nonlinear model of diffusive shock acceleration is applied to the radio light curves of the supernova SN 1993J, which exploded in the nearby galaxy M81. The results of the model suggest that most of the Galactic cosmic rays may be accelerated during the early phase of interaction between the supernova ejecta and the wind lost from the progenitor star.

Supernovae: lights in the darkness (XXIII Trobades Científiques de la Mediterrània)
October 3-5 2007
Mao, Menorca, Spain

[*]Speaker.
[†]Permanent adress: CSNSM, IN2P3-CNRS and Univ Paris-Sud, F-91405 Orsay Cedex, France

PoS(SUPERNOVA)028

1. Introduction

Gamma-ray observations of the Small Magellanic Cloud with the EGRET telescope onboard the *Compton Gamma Ray Observatory* have proved that the bulk of cosmic rays (CRs) propagating in the Milky Way are produced in Galactic sources [1]. Observations of the diffuse γ-ray emission from our Galaxy allow to estimate the total CR luminosity [2]:

$$L_{\rm CR} = L_\gamma \frac{x_\gamma}{x} \sim 5 \times 10^{40} \text{ erg s}^{-1}, \tag{1.1}$$

where $L_\gamma \sim 5 \times 10^{39}$ erg s^{-1} is the total luminosity of diffuse high-energy (> 100 MeV) γ rays emitted in the decay of π^0 produced by CR interaction with the interstellar medium (ISM), $x_\gamma \sim 120$ g cm^{-2} is the mean grammage needed for a CR ion to produce a π^0 in the ISM and $x \sim 12$ g cm^{-2} is the mean path length that CRs traverse before escaping the Galaxy, which is determined from measurements of the CR chemical composition near Earth. In comparison, the total power supplied by Galactic supernovae (SNe) is

$$L_{\rm SN} = E_{\rm SN} R_{\rm SN} \approx 10^{42} \text{ erg s}^{-1}, \tag{1.2}$$

where $E_{\rm SN} \approx 1.5 \times 10^{51}$ erg is the approximate total ejecta kinetic energy of a SN and $R_{\rm SN} \approx 2$ per century is the current epoch Galactic SN rate [3]. Thus, SNe have enough power to sustain the CR population against escape from the Galaxy and energy losses, if there is a mechanism for channeling $\sim 5\%$ of the SN mechanical energy release into relativistic particles.

Diffusive shock acceleration (DSA) at the blast waves generated by SN explosions can in principle produce the required acceleration efficiency, as well as the observed power-law spectrum of CRs [4–7]. In this model, a fraction of ambient particles entering the SN shock front can be accelerated to high energies during the lifetime of a supernova remnant (SNR) by diffusing back and forth on compressive magnetic fluctuations of the plasma flow on both sides of the shock. A critical ingredient of the theory is the strength of the turbulent magnetic field in the shock acceleration region, which governs the acceleration rate and in turn the maximum energy of the accelerated particles. If the turbulent field upstream of the SN shock is similar to the preexisting field in the surrounding ISM ($B \sim 5$ μG), the maximum total energy of an ion of charge Z was estimated 25 years ago to be (for a quasi-parallel shock geometry) $E_{\rm max} \sim 10^{14} Z$ eV [8]. But in more recent developments of the DSA theory, it is predicted that large-amplitude magnetic turbulence is self-generated by streaming of accelerated particles in the shock region, such that the ambient magnetic field can be strongly amplified as part of the acceleration process [9–11]. In this case, protons might be accelerated in SNRs up to 3×10^{15} eV, i.e. the energy of the spectral "knee" above which the measured all-particle CR spectrum shows a significant steepening. Contributions of accelerated α-particles and heavier species might then explain the existing CR measurements up to $\sim 10^{17}$ eV [12]. Above energies of 10^{18}–10^{19} eV, CRs are probably of extragalactic origin.

Another uncertain parameter of the DSA model is the fraction of total shocked particles injected into the acceleration process. Although theoretical progress has been made in recent years [13], the particle injection and consequently the acceleration efficiency are still not well known. However, theory predicts that for efficient acceleration the energy density of the relativistic nuclear component can become comparable to that of the postshock thermal component, in which case the

backreaction of energetic ions can significantly modify the shock structure and the acceleration process can become highly nonlinear (e.g. [14]). In particular, the compression ratio of a CR-modified shock is expected to be higher than for a test-particle shock (i.e. when the accelerated particles have no influence on the shock structure). This is because of both the softer equation of state of a relativistic (CR) gas and the energy loss due to escape of accelerated particles from the shock region [15]. Moreover, the temperature of the shock-heated gas can be reduced if a significant fraction of the total available energy of the shock goes into relativistic particles. Observations of these nonlinear effects [16 – 18] provide indirect evidence for the efficient acceleration of ions in SN shock waves.

The acceleration of electrons in SNRs leaves no doubt, since we observe the nonthermal synchrotron emission that these particles produce in the local magnetic field. Radio synchrotron radiation, which in SNRs is emitted by GeV electrons, was discovered in the 1950's. More recent is the observation of X-ray synchrotron emission from young shell-type SNRs [19], which is due to electrons accelerated to very high energies, $E_e > 1$ TeV. Thanks to the extraordinary spectroscopic-imaging capabilities of the *XMM-Newton* and *Chandra* X-ray observatories, this nonthermal emission can now be studied in great details and recent observations of SNRs with these satellites have shed new light on the DSA rate and the maximum energy of the accelerated particles. This is the subject of Section 2.

In Section 3, we discuss the origin of the TeV γ-ray emission observed from a handful of shell-type SNRs with atmospheric Cerenkov telescopes. For some objects, the detected γ-rays have been explained as resulting from π^0 production in nuclear collisions of accelerated ions with the ambient gas. If this were true, this high-energy emission would be the first observational proof that CR ions are indeed accelerated in SN shock waves. However, the origin of the TeV γ-rays emitted in SNRs is still a matter of debate, because at least in some cases the high-energy photons can also be produced by inverse Compton scattering of cosmic-microwave-background photons (and possibly optical and infrared interstellar photons) by ultrarelativistic electrons.

In Section 4, we show that radio observations of extragalactic SNe can provide complementary information on the DSA mechanism. As an example, we use a semianalytic description of nonlinear DSA to model the radio light curves of SN 1993J. We choose this object because the set of radio data accumulated over the years [20] constitutes one of the most detailed sets of measurements ever established for an extragalactic SN in any wavelength range. We derive from these data constraints on the magnetic field strength in the environment of the expanding SN shock wave, the maximum energy of the accelerated particles, as well as on the fractions of shocked electrons and protons injected into the acceleration process. Conclusions are given in Section 5.

2. X-ray synchrotron emission from SNRs

Together with the thermal, line-dominated X-ray emission from the shock-heated gas, a growing number of SNRs show nonthermal, featureless emission presumably produced by ultrarelativistic electrons in the blast wave region via a synchrotron process. High-angular resolution observations made with the *Chandra* and *XMM-Newton* X-ray observatories have revealed very thin rims of nonthermal emission associated with the forward shock. In several cases, like SN 1006 [19] and G347.3-0.5 [21], the synchrotron component completely dominates the thermal X-ray emis-

sion. The measured power-law spectral index of the X-ray synchrotron radiation is always much steeper than that of the nonthermal radio emission, which is consistent with expectation that the X-ray domain probes the high-energy end of the accelerated electron distribution. The comparison of radio and X-ray fluxes allows to determine the exponential cutoff (maximum) frequency of the synchrotron emission, ν_c, which is related to the maximum energy of the accelerated electrons and the ambient magnetic field as (e.g. [22])

$$\nu_c = 1.26 \times 10^{16} \left(\frac{E_{e,\max}}{10\ \mathrm{TeV}} \right)^2 \left(\frac{B}{10\ \mu\mathrm{G}} \right) \mathrm{Hz}. \tag{2.1}$$

Diffusive shock acceleration can only occur for particles whose acceleration rate is higher than their energy loss rate in the acceleration region. The maximum electron energy, $E_{e,\max}$, can be estimated by equating the synchrotron cooling time (e.g. [23]),

$$\tau_{\mathrm{syn}}(E_{e,\max}) = \frac{E_{e,\max}}{(dE/dt)_{\mathrm{syn}}} \propto E_{e,\max}^{-1} B^{-2}, \tag{2.2}$$

where $(dE/dt)_{\mathrm{syn}}$ is the synchrotron loss rate at $E_{e,\max}$, to the acceleration time

$$\tau_{\mathrm{acc}}(E_{e,\max}) = \frac{E_{e,\max}}{(dE/dt)_{\mathrm{acc}}} \sim \frac{\kappa(E_{e,\max})}{V_s^2}, \tag{2.3}$$

where $(dE/dt)_{\mathrm{acc}}$ and $\kappa(E_{e,\max})$ are the acceleration rate and mean spatial diffusion coefficient of the electrons of energy $E_{e,\max}$ in the blast wave region and V_s is the shock speed. We have neglected here the dependence of τ_{acc} on the shock compression ratio (see [23]). The value of $\kappa(E_{e,\max})$ depends on the strength and structure of the turbulent magnetic field. The DSA theory predicts that CRs efficiently excite large amplitude magnetic fluctuations upstream of the forward shock and that these fluctuations scatter CRs very efficiently [6, 9–11]. It is therefore generally assumed that the spatial diffusion coefficient is close to the Bohm limit:

$$\kappa \gtrsim \kappa_B = \frac{r_g v}{3}, \tag{2.4}$$

where v is the particle speed and r_g=$pc/(QeB)$ the particle gyroradius, p being the particle momentum, c the speed of light, Q the charge number ($Q = 1$ for electrons and protons), and $-e$ the electronic charge. Note that for ultrarelativistic electrons, $\kappa_B = r_g c/3 \propto E_e B^{-1}$. Equating equations (2.2) and (2.3) and using equation (2.1) to express $E_{e,\max}$ as a function of B and ν_c, we can write the ratio of the electron diffusion coefficient at the maximum electron energy to the Bohm coefficient as:

$$\eta_\kappa = \frac{\kappa(E_{e,\max})}{\kappa_B} \propto V_s^2 \nu_c^{-1}. \tag{2.5}$$

Thus, measurements of V_s and ν_c can allow to derive η_κ without knowing the ambient magnetic field. Using this result, several recent studies [22–25] have shown that there are regions in young ($t < 10^4$ yr) SNRs where *acceleration occurs nearly as fast as the Bohm theoretical limit* (i.e. $1 < \eta_\kappa < 10$). This provides an important confirmation of a key prediction of the DSA model.

The strength of the magnetic field in the shock acceleration region may be derived from the thickness of the nonthermal X-ray rims observed in young SNRs (e.g. [26, 27, 23]). One of the two interpretations that have been proposed to explain the thin X-ray filaments is that they result from

fast synchrotron cooling of ultrarelativistic electrons transported downstream of the forward shock. In this scenario, the width of the filaments is set by the distance that the electrons cover before their synchrotron emission falls out of the X-ray band. The electron transport in the downstream region is due to a combination of diffusion and advection, whose corresponding scale heights are [27] $l_{\rm diff} = \sqrt{\kappa \tau_{\rm syn}} \propto B^{-3/2}$ (see eqs.[2.2] and [2.4]) and $l_{\rm adv} = \tau_{\rm syn} V_s / r_{\rm tot} \propto B^{-3/2} E_X^{-1/2} V_s / r_{\rm tot}$, respectively. Here, $r_{\rm tot}$ is the overall compression ratio of the shock and $E_X \sim 5$ keV is the typical X-ray energy at which the rims are observed. Thus, by comparing $l_{\rm diff}$ and $l_{\rm adv}$ to the measured width of the X-ray filaments (e.g. $l_{\rm obs} \approx 3''$ in Cas A which gives 0.05 pc for a distance of 3.4 kpc [26]) one can estimate the downstream magnetic field. Applications of this method to *Chandra* and *XMM-Newton* observations of young SNRs have shown that *the magnetic field at the forward shock is amplified by about two orders of magnitude* as compared with the average Galactic field strength. This conclusion has been recently strengthened by the observations of rapid time variations ($\sim$1 yr) in bright X-ray filaments of the SNR RXJ1713.7-3946 (also named G347.3-0.5), which are interpreted as resulting from fast synchrotron cooling of TeV electrons in a magnetic field amplified to milligauss levels [28]. Such a high magnetic field is likely the result of a nonlinear amplification process associated with the efficient DSA of CRs [9 – 11].

The other interpretation that has been proposed to account for the thin X-ray filaments is that they reflect the spatial distribution of the ambient magnetic field rather than the spatial distribution of the ultrarealtivistic electrons [29]. In this scenario, the magnetic field is thought to be amplified at the shock as well, but the width of the X-ray rims is not set by $l_{\rm diff}$ and $l_{\rm adv}$, but by the damping length of the magnetic field behind the shock. In this case, the relation given above between the rim thickness and the downstream magnetic field would not be valid. Comparison of high-resolution X-ray and radio images could allow to distinguish between the two interpretations, because the synchrotron energy losses are expected to be relatively small for GeV electrons emitting in the radio band [26]. Thus, if the X-ray filaments are due to rapid synchrotron cooling of TeV electrons, the same structures should not be seen in radio images. A recent detailed study of Tycho's SNR has not allowed to draw firm conclusions on the role of magnetic damping behind the blast wave [30]. Further high-resolution observations of SNRs in radio wavelengths would be very useful.

The findings that (1) DSA can proceed at nearly the maximum possible rate (i.e. the Bohm limit) and (2) the magnetic field in the acceleration region can be strongly amplified, suggest that CR ions can reach higher energies in SNR shocks than previously estimated by Lagage & Cesarsky [8]. Thus, Berezhko & Völk [12] have argued that protons can be accelerated in SNRs up to the energy of the knee in the CR spectrum, at 3×10^{15} eV. But relaxing the assumption of Bohm diffusion used in the calculations of Berezhko & Völk, Parizot et al. [23] have obtained lower maximum proton energies for five young SNRs. These authors have derived an upper limit of $\sim 8 \times 10^{14}$ eV on the maximum proton energy, $E_{p,\rm max}$, and have suggested that an additional CR component is required to explain the CR data above the knee energy. Recently, Ellison & Vladimirov [31] have pointed out that the average magnetic field that determines the maximum proton energy can be substantially less than the field that determines the maximum electron energy. This is because electrons remain in the vicinity of the shock where the magnetic field can be strongly amplified, whereas protons of energies $E_p > E_{e,\rm max}$ diffuse farther in the shock precursor region where the field is expected to be weaker ($E_{p,\rm max} > E_{e,\rm max}$ because radiation losses affect the electrons only). This nonlinear effect of efficient DSA could reduce $E_{p,\rm max}$ relative to the value expected from test-

particle acceleration. Nonetheless, recent calculations of $E_{p,\max}$ in the framework of nonlinear DSA models suggest that SNRs might well produce CRs up to the knee [31, 32].

3. TeV gamma-ray emission from SNRs

Atmospheric Cerenkov telescopes have now observed high-energy γ rays from six shell-type SNRs: Cas A with HEGRA [33] and MAGIC [34], RX J1713.7-3946 with CANGAROO [35] and HESS [36], RX J0852.0-4622 (Vela Junior) with CANGAROO-II [37] and HESS [38], RCW 86 with HESS [39], IC 443 with MAGIC [40], and very recently SN 1006 in deep HESS observations [41]. In addition, four γ-ray sources discovered in the Galactic plane survey performed with HESS are spatially coincident with SNRs [42].

With an angular resolution of $\sim 0.06^\circ$ for individual γ rays [36, 38], HESS has provided detailed images above 100 GeV of the extended SNRs RX J1713.7-3946 and RX J0852.0-4622 (their diameters are $\sim 1^\circ$ and $\sim 2^\circ$, respectively). In both cases the images show a shell-like structure and there is a striking correlation between the morphology of the γ-ray emission and the morphology previously observed in X-rays. For both objects the X-ray emission is completely dominated by nonthermal synchrotron radiation. The similarity of the γ-ray and X-ray images thus suggest that the high-energy emission might also be produced by ultrarelativistic electrons, via inverse Compton (IC) scattering off cosmic-microwave-background (CMB), optical-starlight and infrared photons. The γ-ray radiation would then be produced by electrons of energy (in the Thompson limit)

$$E_e \sim \left(\frac{3}{4}\frac{E_\gamma}{E_\star}\right)^{1/2} m_e c^2, \tag{3.1}$$

where $E_\star$ is the typical energy of the seed photons, E_γ is the average final energy of the upscattered photons and m_e is the electron mass. For the CMB, whose contribution to the total IC emission of SNRs generally dominates, $E_\star \sim 3kT_{\rm CMB} = 7.1\times10^{-4}$ eV (k is the Boltzmann constant and $T_{\rm CMB} = 2.73$ K). Significant γ-ray emission beyond $E_\gamma = 30$ TeV has been detected from RX J1713.7-3946 [36]. Thus, an IC origin for the high-energy emission would imply that electrons are accelerated to more than 90 TeV in this object. In more accurate calculations that take into account the contributions of the optical and infrared interstellar radiation fields, the maximum electron energy is found to be $E_{e,\max} \sim 15$–40 TeV [43]. This result is consistent with the value of $E_{e,\max}$ derived from the width of X-ray filaments in RX J1713.7-3946, $E_{e,\max} = 36$ TeV [23].

Assuming that the same population of ultrarelativistic electrons produce both the observed TeV γ-rays and nonthermal X-rays, the mean magnetic field in the interaction region can be readily estimated from the ratio of synchrotron to IC luminosities:

$$\frac{L_{\rm syn}}{L_{\rm IC}} = \frac{U_B}{U_{\rm rad}} = \frac{B^2}{8\pi U_{\rm rad}}, \tag{3.2}$$

where $U_B = B^2/(8\pi)$ is the magnetic field energy density and $U_{\rm rad}$ is the total energy density of the seed photon field. With $U_{\rm CMB} \approx 0.25$ eV cm^{-3} for the CMB and $U_{\rm IR} \approx 0.05$ eV cm^{-3} for the interstellar infrared background (e.g. [44]), we have $U_{\rm rad} \approx 0.3$ eV cm^{-3} (we neglect here the contribution to the IC emission of the optical starlight background). Then, from the measured ratio $L_{\rm syn}/L_{\rm IC} \approx 10$ for RX J1713.7-3946 [44], we obtain $B \approx 11$ μG. This value is significantly lower

than the downstream magnetic field estimated from the observed X-ray rims: $B \sim 80$ μG [23] (or $B > 65$ μG in Ref. [45]). In other words, if the magnetic field in the electron interaction region is as high as derived from the width of the X-ray filaments, IC radiation cannot account for the TeV γ-ray data.

The magnetic field amplification is the main argument to favor a hadronic origin for the high-energy γ rays produced in RX J1713.7-3946 and other SNRs [45]. The shape of the measured γ-ray spectrum below $\sim$1 TeV has also been used to advocate that the high-energy emission might not be produced by IC scattering [44], but the IC calculations of Ref. [43] reproduce the broadband emission of RX J1713.7-3946 reasonably well. In the hadronic scenario, the TeV γ rays are due to nuclear collisions of accelerated protons and heavier particles with ambient ions, which produce neutral pions π^0 that decay in 99% of the cases into two photons with energies of 67.5 GeV each in the π^0 rest frame (2×67.5 GeV is the π^0 mass). At TeV energies in the observer rest frame, the spectrum of the π^0-decay γ rays essentially reproduces, with a constant scaling factor, the one of the parent ultrarelativistic particles. The accelerated proton energies can be estimated from the γ-ray spectrum as $E_p \sim E_\gamma/0.15$ [36]. The detection of γ rays with $E_\gamma > 30$ TeV in RX J1713.7-3946 thus implies that protons are accelerated to more than 200 TeV, which is still about an order of magnitude below the energy of the knee.

However, the hadronic scenario is problematic for RX J1713.7-3946. Due to the lack of thermal X-ray emission, the remnant is thought to expand mostly in a very diluted medium of density $n < 0.02$ cm^{-3} [21]. It is likely that the SN exploded in a bubble blown by the wind of the progenitor star. The flux of γ rays produced by pion decay is proportional to the product of the number of accelerated protons and the ambient medium density. Thus, the total energy contained in CR protons would have to be large to compensate the low density of the ambient medium. From the γ-ray flux measured with HESS from the center of the remnant, Plaga [46] has recently estimated that the total CR-proton energy would have to be $> 4 \times 10^{51}$ erg! Katz & Waxman [47] also argue against a hadronic origin for the TeV emission from RX J1713.7-3946. They show that it would require that the CR electron-to-proton abundance ratio at a given relativistic energy $K_{\rm ep} \lesssim 2 \times 10^{-5}$, which is inconsistent with the limit they derived from radio observations of SNRs in the nearby galaxy M33, $K_{\rm ep} \gtrsim 10^{-3}$. Moreover, radio and X-ray observations of RX J1713.7-3946 suggest that the blast wave has recently hit a complex of molecular clouds located in the western part of the remnant [21]. The ambient medium density in this region has been estimated to be ~ 300 cm^{-3}. In the hadronic scenario, a much higher γ-ray flux would be expected in this direction, contrary to the observations [46]. Thus, the γ-ray morphology revealed by HESS practically rules out pion production as the main contribution to the high-energy radiation of RX J1713.7-3946.

But then, why the magnetic field given by the ratio of synchrotron to IC luminosities (eq. [3.2]) is inconsistent with the field derived from the X-ray filaments? This suggests that the filamentary structures observed with *Chandra* and *XMM-Newton* are localized regions where the magnetic field is enhanced in comparison with the mean downstream field [47]. It is possible that the magnetic field is amplified at the shock as part of the nonlinear DSA process, but then rapidly damped behind the blast wave [29]. The mean field downstream the shock would then not be directly related to the observed thickness of the X-ray rims.

Although the unambiguous interpretation of the TeV observations of shell-type SNRs remains uncertain, the high-energy γ-ray emissions from RX J1713.7-3946 and RX J0852.0-4622 are prob-

ably produced by IC scattering [47]. For Cas A, the case for a hadronic origin of the TeV radiation may be more compelling, as the density of the ambient medium is higher [26]. The new source MAGIC J0616+225 [40] which is spatially coincident with IC 443 may also be produced by pion decay. IC 443 is one of the best candidates for a γ-ray source produced by interactions between CRs accelerated in a SNR and a nearby molecular cloud [48]. Hopefully the upcoming *GLAST* satellite will allow a clear distinction between hadronic and electronic γ-ray processes in these objects. With the expected sensitivity of the LAT instrument between 30 MeV and 300 GeV, *GLAST* observations of SNRs should differentiate between pion-decay and IC spectra [49].

4. Radio emission and nonlinear diffusive shock acceleration in SN 1993J

About 30 extragalactic SNe have now been detected at radio wavelengths[1]. In a number of cases, the radio evolution has been monitored for years after outburst. It is generally accepted that the radio emission is nonthermal synchrotron radiation from relativistic electrons accelerated at the SN shock wave [50]. At early epochs the radio flux can be strongly attenuated by free-free absorption in the wind lost from the progenitor star prior to the explosion. Synchrotron self-absorption can also play a role in some objects [51]. The radio emission from SNe can provide unique information on the physical properties of the circumstellar medium (CSM) and the final stages of evolution of the presupernova system [52]. We show here that this emission can also be used to study critical aspects of the DSA mechanism.

The type IIb SN 1993J, which exploded in the nearby galaxy M81 at a distance of 3.63 ± 0.34 Mpc, is one of the brightest radio SNe ever detected (see [20] and references therein). Very long baseline interferometry (VLBI) imaging has revealed a decelerating expansion of a shell-like radio source, which is consistent with the standard model that the radio emission arises from a region behind the forward shock propagating into the CSM. The expansion has been found to be self-similar [53], although small departures from a self-similar evolution have been reported [54]. The velocity of the forward shock can be estimated from the measured outer radius of the radio shell, i.e. the shock radius r_s, as $V_s = dr_s/dt = 3.35 \times 10^4\ t_d^{-0.17}$ km s^{-1}, where t_d is the time after shock breakout expressed in days.

Extensive radio monitoring of the integrated flux density of SN 1993J has been conducted with the Very Large Array and several other radio telescopes [20]. Figure 1 shows a set of measured light curves at 0.3 cm (85–110 GHz), 1.2 cm (22.5 GHz), 2 cm (14.9 GHz), 3.6 cm (8.4 GHz), 6 cm (4.9 GHz), and 20 cm (1.4 GHz). We see that at each wavelength the flux density first rapidly increases and then declines more slowly as a power in time (the data at 0.3 cm do not allow to clearly identify this behavior). The radio emission was observed to suddenly decline after day $\sim$3100 (not shown in Fig. 1), which is interpreted in terms of an abrupt decrease of the CSM density at radial distance from the progenitor $r \sim 3 \times 10^{17}$ cm [20]. The maximum intensity is reached first at lower wavelengths and later at higher wavelengths, which is characteristic of absorption processes. For SN 1993J, both free-free absorption in the CSM and synchrotron self-absorption are important [51, 55, 20]. To model light curves of radio SNe, Weiler et al. [52, 20] have developed a semi-empirical formula that takes into account these two absorption mechanisms.

[1] See http://rsd-www.nrl.navy.mil/7213/weiler/kwdata/rsnhead.html.

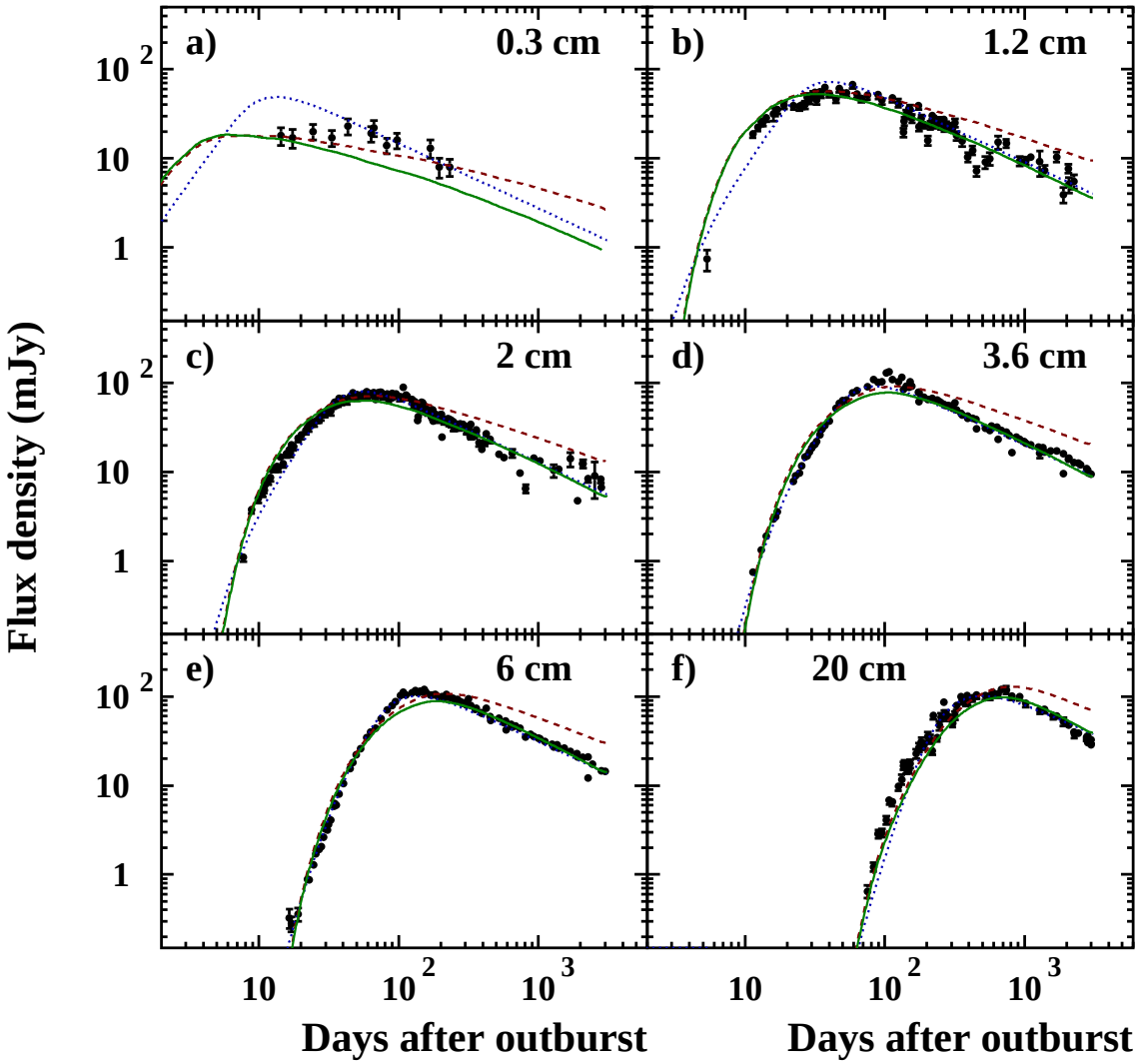

Figure 1: Radio light curves for SN 1993J at 0.3, 1.2, 2, 3.6, 6, and 20 cm. The dotted blue lines represent the best fit semi-empirical model of Ref. [20]. The dashed red (resp. solid green) lines show results of the present model for $\eta^p_{\rm inj} = \eta^e_{\rm inj} = 10^{-5}$ (resp. $\eta^p_{\rm inj} = 2\times10^{-4}$ and $\eta^e_{\rm inj} = 1.4\times10^{-5}$; see text). The data are from Ref. [20] and references therein.

For SN 1993J, the best fit to the data using this semi-empirical model (*dotted blue curves* in Fig. 1) requires nine free parameters [20].

I have developed a model for the radio emission of SN 1993J, which is inspired by previous works on the morphology of synchrotron emission in young SNRs [56, 57]. The model will be presented in detail in a forthcoming publication [58] and I only give here broad outlines. First, the density profile for the CSM is taken as $\rho_{\rm CSM}(r) = \rho_0 (r/r_0)^{-2}$ as expected for a constant wind mass-loss rate and terminal velocity. Here $r_0 = 3.49\times10^{14}$ cm is the shock radius at $t = 1$ day after outburst and ρ_0 is a free parameter. Evidence for a flatter CSM density profile has been advocated ($\rho_{\rm CSM} \propto r^{-s}$, with $s \sim 1.6$; see [20] and references therein), based on the measured time dependence of the optical depth to free-free absorption in the CSM, $\tau_{\rm ff}$. However, Fransson & Björnsson [55]

have shown that the time evolution of $\tau_{\rm ff}$ can be explained by a decrease of the CSM temperature with r together with the standard r^{-2} distribution for the density. The results of the present work provide support to this latter interpretation [58]. Thus, in the present model, free-free absorption is calculated assuming the time dependence of $\tau_{\rm ff}$ obtained in Ref. [55] and using the best-fit value of ρ_0 (or more precisely ρ_0^2) as a normalization factor.

Because synchrotron self-absorption is important in SN 1993J, the strength and evolution of the mean magnetic field in the region of the radio emission can be estimated from the measured peak flux at different wavelengths [51]. Using equation (12) of Ref. [51], I obtain from the data at 1.2, 2, 3.6, 6, and 20 cm:

$$\langle B \rangle = (46 \pm 19) \alpha^{-2/9} t_d^{-1.01 \pm 0.09} \ {\rm G}, \tag{4.1}$$

where α is the ratio of the total energy density in relativistic electrons to the magnetic energy density. The errors include the uncertainty in the contribution of free-free absorption. This time dependence of $\langle B \rangle$ is close to that expected if the magnetic field at the shock is amplified by a constant factor from the available kinetic energy density (see [9]). In this case, one expects $B^2/8\pi \propto \rho_{\rm CSM} V_s^2$, which gives $B \propto t^{-1}$ for $\rho_{\rm CSM} \propto r^{-2}$. Note that the flatter CSM density profile supported by Weiler et al. [20], $\rho_{\rm CSM} \propto r^{-1.6}$, would imply for the assumed scaling $B \propto \rho_{\rm CSM}^{1/2} V_s \propto t^{-0.83}$, which is somewhat inconsistent with the data.

Based on the measured time dependence of $\langle B \rangle$, the immediate postshock magnetic field is assumed to be of the form $B_d = B_0 t_d^{-1}$, where B_0 is a free parameter expected to be in the range $\sim$100–600 G for a typical value of α in the range $\sim 10^{-5}$–10^{-2} (see eq. [4.1]). The evolution of the magnetic field behind the shock is then calculated from the assumption that the field is carried by the flow, frozen in the plasma, so that the parallel and perpendicular magnetic field components evolve conserving flux (see [56] and references therein). Results obtained with the alternative assumption that the magnetic field is rapidly damped behind the shock wave will be given in [58].

The hydrodynamic evolution of the plasma downstream the forward shock is calculated from the two-fluid, self-similar model of Chevalier [59], which takes into account the effects of CR pressure on the dynamics of the thermal gas. The overall structure of SNRs can be described by self-similar solutions, if the initial density profiles in the ejected material (ejecta) and in the ambient medium have power-law distributions, and if the ratio of relativistic CR pressure to total pressure at the shock front is constant [59]. The backreaction of energetic ions can strongly modify the shock structure of young SNRs, such as e.g. Kepler's remnant [15]. But the situation is different for SN 1993J because of the much higher magnetic field in the shock precursor region, which implies that energy is very efficiently transfered from the CRs to the thermal gas via Alfvén wave dissipation [14]. The resulting increase in the gas pressure ahead of the viscous subshock is found to limit the overall compression ratio, $r_{\rm tot}$, to values close to 4 (i.e. the standard value for a test-particle strong shock) even for efficient DSA. Thus, the hydrodynamic evolution of SN 1993J can be safely calculated in the test-particle, self-similar approximation.

Both the energy spectra of the accelerated particles and the thermodynamic properties of the gas just behind the shock front (i.e. the boundary conditions for the self-similar solutions of the hydrodynamic evolution) are calculated with the semianalytic model of nonlinear DSA developed by Berezhko & Ellison [14] and Ellison et al. [60]. However, a small change to the model has been made: the Alfvén waves are assumed to propagate isotropically in the precursor region and

not only in the direction opposite to the plasma flow (i.e. eqs. (52) and (53) of Ref. [14] are not used). This is a reasonable assumption given the strong, nonlinear magnetic field amplification [9]. Although the semianalytic model strictly applies to plane-parallel, steady state shocks, it has been sucessfully used in Ref. [60] for evolving SNRs. The main parameter of this model, $\eta_{\rm inj}^{p}$, is the fraction of total shocked protons in protons with momentum $p \geq p_{\rm inj}$ injected from the postshock thermal pool into the DSA process. The work of Ref. [13] allows us to accurately relate the injection momentum $p_{\rm inj}$ to $\eta_{\rm inj}^{p}$. Similarly, we define $\eta_{\rm inj}^{e}$ for the electron injection. The latter parameter is not important for the shock structure, because the fraction of total particle momentum carried by electrons is negligible, but it determines the brightness of optically-thin synchrotron emission for a given magnetic field strength. The electrons accelerated at the shock experience adiabatic and synchrotron energy losses as they are advected downstream with the plasma flow. The spectral evolution caused by these losses is calculated as in Ref. [61]. Finally, once both the nonthermal electron distribution and the magnetic field in a given shell of material behind the forward shock have been determined, the synchrotron emission from that shell can be calculated [62]. The total radio emission along the line of sight is then obtained from full radiative transfer calculations that include synchrotron self-absorption.

With the set of assumptions given above, the model has four free parameters: ρ_0, B_0, $\eta_{\rm inj}^{p}$ and $\eta_{\rm inj}^{e}$. While the product $\rho_0 \times \eta_{\rm inj}^{e}$ is important for the intensity of optically-thin synchrotron emission, the CSM density normalization ρ_0 also determines the level of free-free absorption. The main effect of changing B_0 is to shift the radio light curves in time, because the turn-on from optically-thick to optically-thin synchrotron emission is delayed when the magnetic field is increased. The proton injection paramater $\eta_{\rm inj}^{p}$ determines the shock structure and hence influences the shape of the electron spectrum.

Calculated radio light curves are shown in Fig. 1 for $\rho_0 = 1.8 \times 10^{-15}$ g cm^{-3}, $B_0 = 400$ G, and two sets of injection parameters: $\eta_{\rm inj}^{p} = \eta_{\rm inj}^{e} = 10^{-5}$ (test-particle case), and $\eta_{\rm inj}^{p} = 2 \times 10^{-4}$ and $\eta_{\rm inj}^{e} = 1.4 \times 10^{-5}$. We see that in the test-particle case, the decline of the optically-thin emission with time is too slow as compared to the data, except at 0.3 cm. The CR-modified shock provides a better overall fit to the measured flux densities, although significant deviations from the data can be observed. In particular, we see that the calculated light curve at 0.3 cm falls short of the data at this wavelength. It is possible that the deviations of the best-fit curves from the data partly arise from the approximations used in the DSA model of Ref. [14], in which the nonthermal phase-space distribution function $f(p)$ is described as a three-component power law. But it is also possible that it tells us something about the magnetic field evolution in the downstream region. The spatial distribution of the postshock magnetic field will be studied in Ref. [58] by comparing calculated synchrotron profiles with the observed average profile of the radio shell.

For SN 1993J, the main effect of the CR pressure is to reduce the compression ratio of the subshock, $r_{\rm sub}$, whereas the overall compression ratio $r_{\rm tot}$ remains nearly constant (see above). For $\eta_{\rm inj}^{p} = 2 \times 10^{-4}$, $r_{\rm sub}$ is found to decrease from 3.58 to 3.35 between day 10 and day 3100 after outburst, whereas $r_{\rm tot}$ stays between 4 and 4.04. Such a shock modification affects essentially the particles of energies $< m_p c^2$ that remain in the vicinity of the subshock during the DSA process. Thus, we see in Fig. 2 that the increase of $\eta_{\rm inj}^{p}$ from 10^{-5} to 2×10^{-4} steepens the phase-space distribution functions $f(p)$ of both protons and electrons between their thermal Maxwell-Boltzmann distributions and ~ 1 GeV, as the spectral index in this energy domain, $q_{\rm sub} = 3r_{\rm sub}/(r_{\rm sub} - 1)$ with

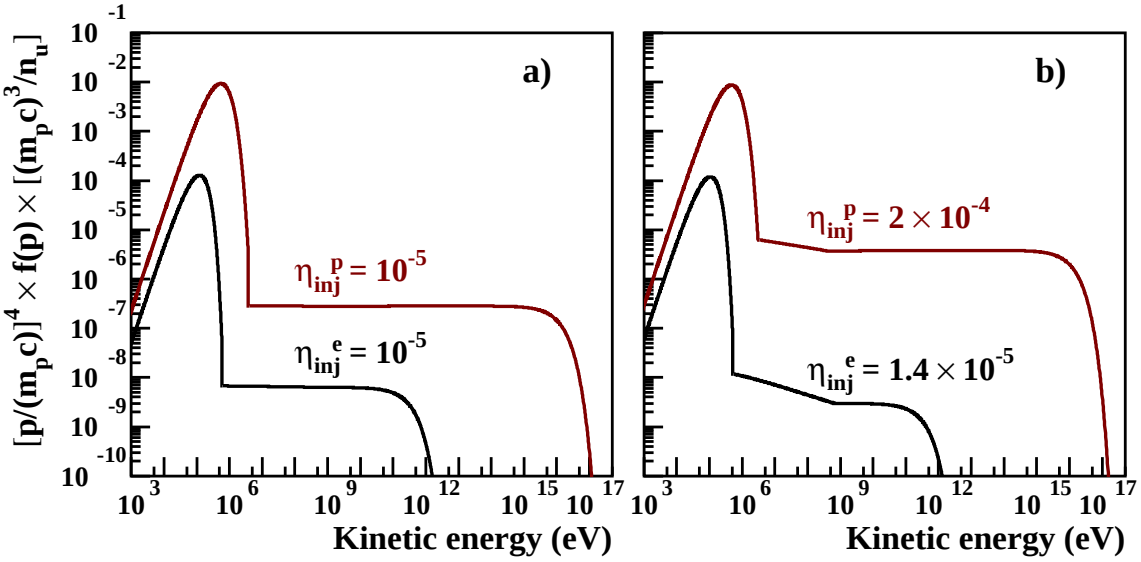

Figure 2: Calculated postshock phase space distribution functions, $f(p)$, vs. kinetic energy, at day 100 after shock breakout. Following Ref. [14], $f(p)$ has been multiplied by $[p/(m_p c)]^4$ to flatten the spectra, and by $[(m_p c)^3/n_u]$ to make them dimensionless (m_p is the proton mass and n_u the proton number density ahead of the shock precursor). The red lines are for protons and the black lines for electrons. The two sets of injection parameters $\eta_{\rm inj}^p$ and $\eta_{\rm inj}^e$ are those used for the synchrotron calculations shown in Fig. 1.

$f(p) \propto p^{-q_{\rm sub}}$ [14], increases with decreasing $r_{\rm sub}$. The radio light curves provide clear evidence that the spectral index of the nonthermal electrons below 1 GeV is higher than the strong-shock test-particle value $q_{\rm sub} = 4$. For the preferred injection parameters $\eta_{\rm inj}^p = 2 \times 10^{-4}$ and $\eta_{\rm inj}^e = 1.4 \times 10^{-5}$, the calculated electron-to-proton ratio at, e.g., 10 GeV is $K_{\rm ep} = 7.8 \times 10^{-4}$ at $t_d = 100$ days (Fig. 2) and $K_{\rm ep} = 6.3 \times 10^{-4}$ at $t_d = 3100$ days. These values are roughly consistent with – but slightly lower than – those recently estimated for the blast wave of Tycho's SNR, $K_{\rm ep} \sim 10^{-3}$ [30].

The immediate postshock magnetic field obtained in this work, $B_d \approx 400 \times t_d^{-1}$ G is in very good agreement with the mean field in the synchrotron-emitting region previously estimated by Fransson & Björnsson [55], $\langle B \rangle \approx 370 \times t_d^{-1}$ G. As already pointed out by Bell & Lucek [9], the derived magnetic field strength in the forward shock precursor is consistent with a simple estimate based on nonlinear magnetic field amplification driven by the pressure gradient of accelerated particles. For $\eta_{\rm inj}^p = 2 \times 10^{-4}$, the ratio of the mean magnetic energy density in the shock precursor to the energy density in CR protons is found to slightly decrease from 0.6 to 0.5 between day 10 and day 3100 after outburst [58]. It is interesting that the magnetic field strength is very close to that given by equipartition.

As also pointed out in Ref. [9], CRs were probably accelerated to very high energies in SN 1993J short after shock breakout. The maximum proton energy $E_{p,\rm max}$ is expected to be limited by the spatial extend of the shock, because high-energy particles diffusing upstream far enough from the shock front can escape from the acceleration region. This size limitation can be estimated by assuming the existence of an upstream free escape boundary located at some constant fraction $f_{\rm esc}$ of the shock radius: $d_{\rm FEB} = f_{\rm esc} r_s$. The maximum energy that particles can acquire before reaching this boundary is then obtained by equalling $d_{\rm FEB}$ to the upstream diffusion length,

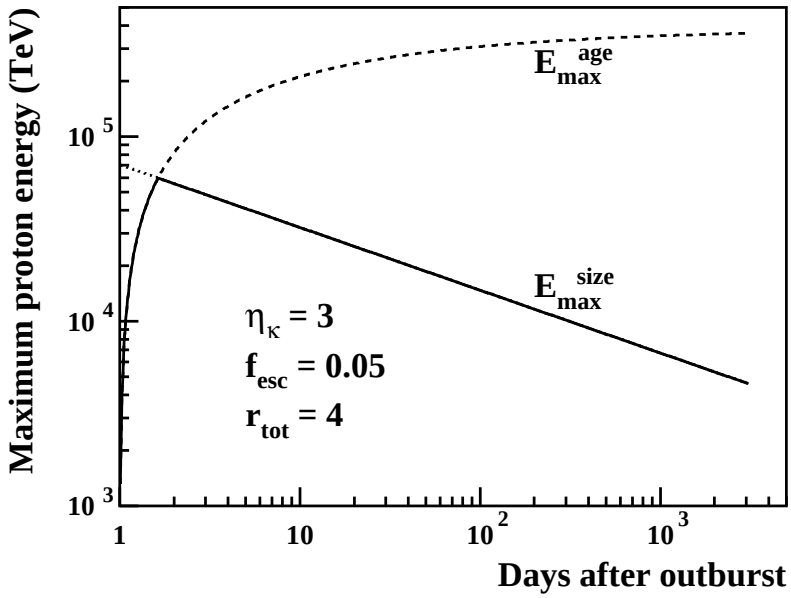

Figure 3: Estimated maximum proton energy in SN 1993J as a function of time after shock breakout. $E_{\rm max}^{\rm age}$ and $E_{\rm max}^{\rm size}$ are the maximum energies caused by the finite shock age and size, respectively. The resulting maximum proton energy (*solid line*) is the minimum of these two quantities.

$l \sim \kappa/V_s$ (e.g. [31]). Calculated time evolution of $E_{p,\rm max}$ is shown in Fig. 3 for $f_{\rm esc} = 0.05$ (see, e.g., [57]) and $\eta_\kappa = 3$ (see eq. 2.5 and, e.g., [23]). We see that the maximum energy caused by the particle escape, $E_{\rm max}^{\rm size}$ ($\propto f_{\rm esc}\eta_\kappa^{-1}$), becomes rapidly lower than the maximum energy associated with the shock age, $E_{\rm max}^{\rm age}$ ($\propto \eta_\kappa^{-1}$), which is obtained by time integration of the acceleration rate $(dE/dt)_{\rm acc}$ from an initial acceleration time assumed to be $t_0 = 1$ day after outburst. The resulting maximum proton energy (i.e. the minimum of $E_{\rm max}^{\rm size}$ and $E_{\rm max}^{\rm age}$) is significantly lower than the previous estimate of Ref. [9], $E_{p,\rm max} \sim 3\times10^{17}$ eV. Moreover, we did not take into account the nonlinear effects recently pointed out by Ellison & Vladimirov [31], which could further reduce $E_{p,\rm max}$. However, SN 1993J may well have accelerated protons above the knee energy of 3×10^{15} eV (Fig. 3), which provides support to the scenario first proposed by Völk & Biermann [63] that the highest-energy Galactic CRs are produced by massive stars exploding into their own wind. In this context, it is instructive to estimate the total energy acquired by the CR particles during the early phase of interaction between the SN ejecta and the red supergiant wind:

$$E_{\rm CR} \cong \int_{t_d=1}^{3100} \varepsilon_{\rm CR}(t) \times \frac{1}{2}\rho_{\rm CSM}(r_s)V_s^3 \times 4\pi r_s^2 dt = 6.8\times10^{49}\ {\rm erg}, \tag{4.2}$$

where $\varepsilon_{\rm CR}(t)$ is the time-dependent fraction of total incoming energy flux, $F_0(r_s) \cong 0.5\rho_{\rm CSM}(r_s)V_s^3$, going into CR particles. With the best-fit parameters obtained from the radio light curves, $\varepsilon_{\rm CR}(t)$ is found to slowly increase from 12% to 16% between day 10 and day 3100 after outburst. It is remarkable that the value obtained for $E_{\rm CR}$ is very close to the mean energy per SN required to account for the Galactic CR luminosity, $\approx 7.5\times10^{49}$ erg (see Sect. 1), which suggests that SN 1993J might be typical of the SNe that produce the CR population in our own Galaxy.

5. Conclusions

Observations of young shell-type SNRs with the *Chandra* and *XMM-Newton* X-ray space observatories give more credit to the current paradigm that the bulk of Galactic CRs are accelerated in shock waves generated by SN explosions. Evidence is accumulating suggesting that acceleration in SN shocks can be nearly as fast as the Bohm limit and that self-excited turbulence in the shock vicinity can strongly amplify the ambient magnetic field, thus allowing the acceleration of CR ions to energies above 10^{15} eV. Besides, observations of nonlinear effects caused by efficient DSA support the fact that the acceleration efficiency can be high enough to account for the Galactic CR luminosity. But the direct and unambiguous observation of ion acceleration in SN shocks remains uncertain, as it is difficult at the present time to distinguish between pion decay and IC scattering as the main mechanism responsable for the very-high-energy γ-ray emission detected with ground-based atmospheric Cerenkov telescopes from several shell-type SNRs. Following Refs. [46, 47] I have argued, however, that the TeV γ rays emitted in RX J1713.7-3946 and RX J0852.0-4622 are probably produced by ultrarelativistic electrons, via IC scattering off CMB, optical-starlight and infrared photons. One of the most critical ingredients for the interpretation of these observations is the evolution of the postshock magnetic field in the downstream region (see Sect. 3). Hopefully, the upcoming GLAST satellite (launch scheduled for May 2008) will allow a clear identification of the contributions of hadronic and electronic γ-ray emission processes in SNRs, which in turn will be useful to understand the importance of magnetic field damping behind the forward shock.

Radio observations of extragalactic SNe can also shed light on the DSA process. The impressive set of radio data available for SN 1993J make this object a unique laboratory to study particle acceleration in a SN shock. Using a semianalytic model of nonlinear DSA to explain the radio light curves, the results I have obtained suggest, in particular, that the acceleration of ions has become efficient soon after outburst and that the magnetic field in the forward shock vicinity has been amplified to equipartition with the CR energy density. The field amplification implies that CR protons may have been accelerated to energies above 3×10^{15} eV during the early phase of interaction between the SN ejecta and the red supergiant wind lost from the progenitor star. During this time, which lasted only $\sim$8.5 years, the shock processed in the expansion a total energy of 4.6×10^{50} erg and the mean acceleration efficiency was found to be $\varepsilon_{\rm CR} = 15\%$. Thus, a total energy of almost 7×10^{49} erg has been stored up by CR particles during this phase. A significant fraction of this energy might have escaped into the interstellar medium after day $\sim$3100, when the shock started to expand into a more diluted CSM.

The results obtained for SN 1993J suggest that massive stars exploding into a wind environment could be a major source of Galactic CRs, as first proposed by Völk & Biermann [63]. It is well known that most massive stars are born in OB associations, whose activity formes superbubbles of hot and turbulent gas inside which the majority of core-collapse SNe explode. Turbulent re-acceleration inside superbubbles may modify the spectrum of CRs and, in particular, increase their maximum energy (see [64] and references therein).

Acknowledgements

It is a pleasure to thank Anne Decourchelle and Jürgen Kiener for critical reading of the manus-

cipt, Margarita Hernanz for numerous discussions and her hospitality at IEEC-CSIC, and Jordi Isern for the invitation to the conference. Financial support from the Generalitat de Catalunya through the AGAUR grant 2006-PIV-10044 and the project SGR00378 is acknowledged.

References

[1] P. Sreekumar et al., *Phys. Rev. Lett.* **70** (1993) 127

[2] V. A. Dogiel, V. Schönfelder, & A. W. Strong, *Astrophys. J.* **572** (2002) L157

[3] K. Ferrière, *Astrophys. J.* **497** (1998) 759

[4] G. F. Krymskii, *Dokl. Akad. Nauk SSSR* **234** (1977) 1306

[5] W. I. Axford, E. Leer, & G. Skadron, in *Proc. 15th Int. Cosmic-Ray Conf.* (Plovdiv) **11** (1978) 132

[6] A. R. Bell, *Mon. Not. R. Astron. Soc.* **182** (1978) 147

[7] R. D. Blandford & J. Ostriker, *Astrophys. J.* **221** (1978) L29

[8] P. O. Lagage & C. J. Cesarsky, *Astron. Astrophys.* **125** (1983) 249

[9] A. R. Bell & S. G. Lucek, *Mon. Not. R. Astron. Soc.* **327** (2001) 433

[10] E. Amato & P. Blasi, *Mon. Not. R. Astron. Soc.* **371** (2006) 1251

[11] A. Vladimirov, D. C. Ellison, & A. Bykov *Astrophys. J.* **652** (2006) 1246

[12] E. G. Berezhko & H. J. Völk, *Astrophys. J.* **661** (2007) L175

[13] P. Blasi, S. Gabici, & G. Vannoni, *Mon. Not. R. Astron. Soc.* **361** (2005) 907

[14] E. G. Berezhko & D. C. Ellison, *Astrophys. J.* **526** (1999) 385

[15] A. Decourchelle, D. C. Ellison, & J. Ballet *Astrophys. J.* **543** (2000) L57

[16] J. P. Hughes, C. E. Rakowski, & A. Decourchelle, *Astrophys. J.* **543** (2000) L61

[17] A. Decourchelle, in *X-Ray and Radio Connections* (eds. L.O. Sjouwerman and K.K. Dyer), Published electronically by NRAO, http://www.aoc.nrao.edu/events/xraydio, 2005

[18] J. S. Warren et al., *Astrophys. J.* **634** (2005) 376

[19] K. Koyama et al., *Nature* **378** (1995) 255

[20] K. Weiler et al., *Astrophys. J.* **671** (2007) 1959

[21] G. Cassam-Chenaï et al., *Astron. Astrophys.* **427** (2004) 199

[22] M. D. Stage, G. E. Allen, J. C. Houck, & J. E. Davis, *Nature Phys.* **2** (2006) 614

[23] E. Parizot, A. Marcowith, J. Ballet, & Y. A. Gallant, *Astron. Astrophys.* **453** (2006) 387

[24] S. P. Reynolds, *Adv. Space Res.* **33** (2004) 461

[25] R. Yamazaki, T. Yoshida, T. Terasawa, A. Bamba, & K. Koyama, *Astron. Astrophys.* **416** (2004) 595

[26] J. Vink & J. M. Laming, *Astrophys. J.* **584** (2003) 758

[27] J. Ballet, *Adv. Space Res.* **37** (2006) 1902

[28] Y. Uchiyama, F. A. Aharonian, T. Tanaka, T. Takahashi, & Y. Maeda, *Nature* **449** (2007) 576

[29] M. Pohl, H. Yan, & A. Lazarian, *Astrophys. J.* **626** (2005) L101

[30] G. Cassam-Chenaï, J. P. Hughes, J. Ballet, & A. Decourchelle, *Astrophys. J.* **665** (2007) 315

[31] D. C. Ellison & A. Vladimirov, *Astrophys. J.* **673** (2008) L47

[32] P. Blasi, E. Amato, & D. Caprioli, *Mon. Not. R. Astron. Soc.* **375** (2007) 1471

[33] F. Aharonian et al., *Astron. Astrophys.* **370** (2001) 112

[34] J. Albert et al., *Astron. Astrophys.* **474** (2007) 937

[35] R. Enomoto et al., *Nature* **416** (2002) 823

[36] F. Aharonian et al., *Astron. Astrophys.* **464** (2007) 235

[37] H. Katagiri et al., *Astrophys. J.* **619** (2005) L163

[38] F. Aharonian et al., *Astrophys. J.* **661** (2007) 236

[39] S. Hoppe & M. Lemoine-Goumard for the HESS collaboration, in *Proc. 30th Int. Cosmic-Ray Conf.*, in press, arXiv:0709.4103

[40] J. Albert et al., *Astrophys. J.* **664** (2007) L87

[41] F. Aharonian et al., in preparation

[42] F. Aharonian et al., *Astrophys. J.* **636** (2006) 777

[43] T. A. Porter, I. V. Moskalenko, & A. W. Strong, *Astrophys. J.* **648** (2006) L29.

[44] F. Aharonian et al., *Astron. Astrophys.* **449** (2006) 223

[45] E. G. Berezhko & H. J. Völk, *Astron. Astrophys.* **451** (2006) 981

[46] R. Plaga, *New Astron.* **13** (2008) 73

[47] B. Katz & E. Waxman, *J. Cosmology Astropart. Phys.* **01** (2008) 18

[48] D. F. Torres, G. E. Romero, T. M. Dame, J. A. Combi, & Y. M. Butt, *Phys. Rep.* **382** (2003) 303

[49] S. Funk, *Adv. Space Res.* **41** (2008) 464

[50] R. A. Chevalier, *Astrophys. J.* **259** (1982) 302

[51] R. A. Chevalier, *Astrophys. J.* **499** (1998) 810

[52] K. W. Weiler, N. Panagia, M. J. Montes, & R. A. Sramek, *Annu. Rev. Astron. Astrophys.* **40** (2002) 387

[53] J. M. Marcaide et al., *Astrophys. J.* **486** (1997) L31

[54] N. Bartel et al., *Science* **287** (2000) 112

[55] C. Fransson & C.-I. Björnsson, *Astrophys. J.* **509** (1998) 861

[56] G. Cassam-Chenaï, A. Decourchelle, J. Ballet, & D. C. Ellison, *Astron. Astrophys.* **443** (2005) 955

[57] D. C. Ellison & G. Cassam-Chenaï, *Astrophys. J.* **632** (2005) 920

[58] V. Tatischeff, in preparation

[59] R. A. Chevalier, *Astrophys. J.* **272** (1983) 765

[60] D. C. Ellison, E. G. Berezhko, & M. G. Baring, *Astrophys. J.* **540** (2000) 292

[61] S. P. Reynolds, *Astrophys. J.* **493** (1998) 375

[62] A. G. Pacholczyk, *Radio Astrophysics*, San Francisco: Freeman, 1970

[63] H. J. Völk & P. L. Biermann, *Astrophys. J.* **333** (1988) L65

[64] E. Parizot, A. Marcowith, E. van der Swaluw, A. M. Bykov, and V. Tatischeff, *Astron. Astrophys.* **424** (2004) 747